TẠP CHÍ ISSN: 1859-316X, e-ISSN: 3093-3161
KHOA HỌC CÔNG NGHỆ HÀNG HẢI
JOURNAL OF MARINE SCIENCE AND TECHNOLOGY

ADAPTIVE NEURAL NETWORK-ASSISTED LINEAR QUADRATIC REGULATOR CONTROL WITH FULL-ORDER EXTENDED STATE OBSERVER FOR ACTIVE SUSPENSION SYSTEMS

TUAN ANH NGUYEN[1,2*], THI THU HUONG[2], THE TRUC NGUYEN[2], MANH LONG NGUYEN[3], QUANG VINH TRAN[3]

[1]Faculty of Mechanical Engineering, Thuyloi University

[2]School of Mechanical Engineering, Hanoi University of Science and Technology

[3]Phenikaa School of Engineering, Phenikaa University

**Corresponding email: anhngtu@tlu.edu.vn; Anh.NT240065D@sis.hust.edu.vn*

DOI: https://doi.org/10.65154/jmst.1133

Abstract

This paper proposes integrating a Linear Quadratic Regulator (LQR) control scheme with an adaptive Neural Network (NN) updating law to improve ride comfort performance. The dynamic states of the suspension system are effectively estimated using a Full-Order Extended State Observer (FOESO) rather than through direct sensor measurements, thereby reducing implementation costs and minimizing the influence of sensor noise. Numerical simulations are conducted under two different road profile scenarios based on ISO standards, while accounting for lumped uncertainties in the system dynamic modeling. The results show that the Root Mean Square (RMS) body displacement is reduced to 4.854 mm in the first case with ISO C-class road disturbance, and the RMS body acceleration decreases to 0.220 m/s² in the second case with ISO D-class road disturbance; both are significantly lower than those achieved by conventional controllers. Furthermore, the dynamic states are estimated with high accuracy, confirming the effectiveness of the proposed control strategy in suspension system regulation.

Keywords: *Active suspension, Linear quadratic regulator, Neural network, Extended state observer.*

1. Introduction

The suspension system plays an important role in ensuring ride comfort when a vehicle travels over uneven road surfaces. The structure of a passive suspension system is relatively simple, consisting mainly of springs, dampers, and upper or lower control arms. However, such a configuration is often unable to provide satisfactory ride comfort under various complex operating conditions. In recent years, active suspension systems have been increasingly adopted in modern vehicles due to their superior vibration-suppression capabilities, thereby significantly improving ride comfort [1].

Numerous studies on active suspension control have been reported, mainly focusing on the design and improvement of controllers to satisfy system adaptability requirements [2]. Tran et al. [3] designed a Proportional-Integral-Derivative (PID) controller to regulate the performance of an active suspension system, accounting for the hydraulic actuator's influence. Hoang et al. [4] applied a fuzzy logic algorithm to tune PID controller parameters to enhance system responsiveness and adaptability. However, PID control is generally more suitable for single-input single-output systems and may become less effective when dealing with more complex multi-state suspension dynamics.

To overcome this limitation, Vu and Le [5] proposed applying LQR control to suspension models with multiple state variables. The objective of LQR control is to achieve optimal system performance by minimizing a quadratic cost function that balances ride comfort and control effort [6]. However, LQR control requires full-state information for feedback gain calculation, which often requires multiple expensive physical sensors and may introduce sensor noise, thereby reducing the quality of the feedback signal. In addition, lumped uncertainties can compromise the suspension system's stability and degrade ride comfort under practical operating conditions. These effects are often insufficiently considered in studies related to LQR-based suspension control [7, 8].

In this paper, an integrated control strategy combining LQR with an adaptive NN updating law is proposed to improve vibration suppression performance and enhance system robustness against uncertainties. A FOESO is incorporated to estimate the suspension system's dynamic states rather than relying on direct sensor measurements, thereby reducing implementation costs and minimizing the influence of sensor noise. This combination provides a novel approach to addressing the existing limitations of conventional LQR-based suspension control methods.

Compared with existing FOESO-LQR or NN-based suspension control approaches, the proposed method combines FOESO-based full-state estimation with adaptive RBFNN uncertainty compensation within an LQR control framework. The FOESO reduces sensor dependency and measurement noise effects, while the adaptive RBFNN improves robustness against lumped uncertainties and nonlinear disturbances. This integrated structure enhances ride comfort and vibration suppression performance under severe road excitations.

This paper is organized into four sections. Section 1 discusses literature review and identifies the research gaps. Section 2 presents the dynamic model of the suspension system and the controller design procedure. Simulation results and performance evaluations are discussed in Section 3. Finally, important conclusions and future research directions are presented in the Conclusion section.

2. Mathematical models

A quarter-car model of the active suspension system is illustrated in Figure 1, where zs denotes the sprung mass displacement, *zu* denotes the unsprung mass displacement, and *zr* denotes the road disturbance input.

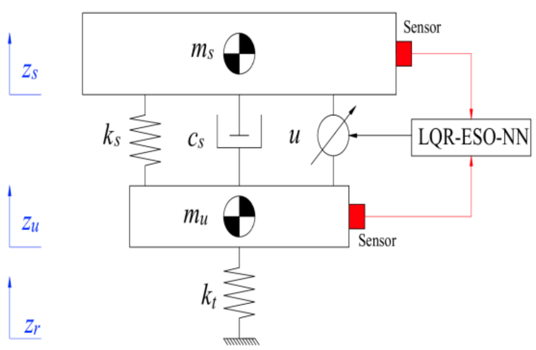

Figure 1. Active suspension model

The suspension system dynamics are described by equations (1) and (2), where ms is the sprung mass, mu is the unsprung mass, d_s denotes the sprung mass lumped uncertainty, d_u represents the unsprung mass lumped uncertainty, and u is the control force generated by the actuator.

$$m_s \ddot{z}_s = F_{ks} + F_{cs} + d_s + u \tag{1}$$

$$m_u \ddot{z}_u = F_{kt} - F_{ks} - F_{cs} + d_u - u \tag{2}$$

The suspension spring force (F_{ks}), suspension damping force (F_{cs}), and tire spring force (F_{kt}) are defined by equations (3)-(5), where k_s is the suspension spring stiffness, c_s is the damping coefficient, and k_t denotes the tire stiffness.

$$F_{ks} = k_s \left(z_u - z_s \right) \tag{3}$$

$$F_{cs} = c_s \left(\dot{z}_u - \dot{z}_s \right) \tag{4}$$

$$F_{kt} = k_t \left(z_r - z_u \right) \tag{5}$$

The state variables are defined in the order presented in equation (6).

$$\begin{bmatrix} x_1 & x_2 & x_3 & x_4 \end{bmatrix}^T = \begin{bmatrix} z_s & \dot{z}_s & z_u & \dot{z}_u \end{bmatrix}^T \tag{6}$$

The suspension system dynamics can be rewritten in matrix form as shown in equation (7),

$$\left[\dot{x}\right] = \boldsymbol{A}\left[x\right] + \boldsymbol{B}\left[u\right] + \boldsymbol{E}\left[z_r\right] \tag{7}$$

Where the matrices ***A***, ***B***, and ***E*** are defined as follows:

$$A = \begin{bmatrix} 0 & 1 & 0 & 0 \\ -\dfrac{k_s}{m_s} & -\dfrac{c_s}{m_s} & \dfrac{k_s}{m_s} & \dfrac{c_s}{m_s} \\ 0 & 0 & 0 & 1 \\ \dfrac{k_s}{m_u} & \dfrac{c_s}{m_u} & -\dfrac{k_s + k_t}{m_u} & -\dfrac{c_s}{m_u} \end{bmatrix} \quad B = \begin{bmatrix} 0 \\ \dfrac{1}{m_s} \\ 0 \\ -\dfrac{1}{m_u} \end{bmatrix}$$

$$E = \begin{bmatrix} 0 & 0 & 0 & \dfrac{k_t}{m_u} \end{bmatrix}^T$$

A FOESO is developed in this study to estimate dynamic state variations rather than relying on direct sensor measurements. The structure of the proposed FOESO is presented in equation (8).

$$\left[\dot{\hat{x}}\right] = \boldsymbol{A}_{ESO}\left[\hat{x}\right] + \boldsymbol{B}_{ESO}\left[u\right] + \boldsymbol{L}\left(\boldsymbol{y} - \boldsymbol{C}_{DO}\left[\hat{x}\right]\right) \tag{8}$$

The observer matrices are defined as follows:

TẠP CHÍ ISSN: 1859-316X, e-ISSN: 3093-3161
KHOA HỌC CÔNG NGHỆ HÀNG HẢI
JOURNAL OF MARINE SCIENCE AND TECHNOLOGY

$$A_{DO} = \begin{bmatrix} 0 & 1 & 0 & 0 & 0 & 0 \\ -\frac{k_s}{m_s} & -\frac{c_s}{m_s} & \frac{k_s}{m_s} & \frac{c_s}{m_s} & 1 & 0 \\ 0 & 0 & 0 & 1 & 0 & 0 \\ \frac{k_s}{m_u} & \frac{c_s}{m_u} & -\frac{k_s+k_t}{m_u} & -\frac{c_s}{m_u} & 0 & 1 \\ 0 & 0 & 0 & 0 & 0 & 0 \\ 0 & 0 & 0 & 0 & 0 & 0 \end{bmatrix}$$

$$B_{DO} = \begin{bmatrix} 0 & \frac{1}{m_s} & 0 & -\frac{1}{m_u} & 0 & 0 \end{bmatrix}^T$$

$$C_{DO} = \begin{bmatrix} 1 & 0 & 0 & 0 & 0 & 0 \\ 0 & 0 & 1 & 0 & 0 & 0 \end{bmatrix}^T$$

To generate the control force, an LQR is designed based on the state-space representation of the suspension system described in equation (7). The control objective is to minimize vehicle body vibration while maintaining suspension stability and ride comfort. The state feedback control law is defined as in (9), where K is the optimal feedback gain matrix obtained from the LQR design.

$$u_{LQR} = -K[\hat{x}] \tag{9}$$

The optimal gain matrix is determined by minimizing the quadratic performance index by (10), where $\boldsymbol{Q}$ is the positive semi-definite weighting matrix associated with the state variables, and $\boldsymbol{R}$ is the positive definite weighting matrix associated with the control input. The selection of $\boldsymbol{Q}$ and $\boldsymbol{R}$ directly affects the trade-off between ride comfort and control effort. The weighting matrices $\boldsymbol{Q}$ and $\boldsymbol{R}$ were selected through iterative simulation-based tuning to achieve a trade-off between ride comfort and control effort. Higher weights were assigned to the sprung mass displacement and acceleration states to prioritize vibration suppression performance, while a relatively small value of $\boldsymbol{R}$ was selected to allow sufficient actuator control force.

$$J = \int_0^\infty \left([\hat{x}]^T \boldsymbol{Q} [\hat{x}] + [u]^T \boldsymbol{R} [u] \right) dt \tag{10}$$

After several simulation tests, the matrices were selected as:

$$\boldsymbol{Q} = diag\begin{bmatrix} 10^0 & 10^0 & 10^2 & 10^4 \end{bmatrix} \quad \boldsymbol{R} = 10^{-3}$$

The optimal feedback gain matrix is calculated as in (11), where $\boldsymbol{P}$ is the positive definite solution of the continuous-time Algebraic Riccati Equation, determined by (12).

$$\boldsymbol{K} = \boldsymbol{R}^{-1}\boldsymbol{B}^T\boldsymbol{P} \tag{11}$$

$$\boldsymbol{A}^T\boldsymbol{P} + \boldsymbol{P}\boldsymbol{A} - \boldsymbol{P}\boldsymbol{B}\boldsymbol{R}^{-1}\boldsymbol{B}^T\boldsymbol{P} + \boldsymbol{Q} = 0 \tag{12}$$

To further compensate for model uncertainties and external disturbances, an adaptive Radial Basis Function Neural Network (RBFNN) is incorporated into the control framework. The NN is employed to estimate the unknown nonlinear dynamics and lumped uncertainties that the conventional LQR controller cannot fully address. The final control input applied to the active suspension actuator is designed as in (13).

$$u = u_{LQR} - u_{NN} \tag{13}$$

The input vector of the RBFNN is selected by (14).

$$[\hat{x}] = [\hat{x}_1 \quad \hat{x}_2 \quad \hat{x}_3 \quad \hat{x}_4] \tag{14}$$

The hidden layer of the neural network consists of N radial basis neurons, and the Gaussian basis function of the i^{th} neuron is defined as in (15), where C_i is the center vector of the i^{th} neuron, and b is the width parameter of the Gaussian function.

$$\Phi_i([\hat{x}]) = \exp\left(-\frac{\left\| [\hat{x}] - C_i \right\|^2}{2b^2} \right) \quad i = \overline{1, N} \tag{15}$$

The basis function vector is expressed as in (16).

$$\Phi([\hat{x}]) = [\Phi_1 \quad \Phi_2 \quad \ldots \quad \Phi_N]^T \tag{16}$$

The neural network compensation signal is calculated by (17), where k_{NN} is the neural network gain, and W is the adaptive weight vector.

$$u_{NN} = k_{NN}\hat{W}^T\Phi([\hat{x}]) \tag{17}$$

To ensure online adaptation and improve approximation performance, the weight updating law is designed according to (18), where Γ is the positive definite adaptation gain matrix, e is the tracking error used for network learning, and σ is the leakage factor introduced to improve robustness and prevent parameter drift.

$$\dot{\hat{W}} = \Gamma\Phi([\hat{x}])e - \sigma\hat{W} \tag{18}$$

In this study, the RBFNN consists of 5 hidden neurons. The center vectors are distributed across the operating region of the suspension states to improve approximation capability, while the Gaussian width parameter is set to b=5. The adaptation gain matrix is selected as $\Gamma=100\boldsymbol{I}$ to ensure sufficiently fast convergence and online learning performance without causing excessive oscillations in the adaptive weights. In addition, the leakage factor is set to $\sigma=5$ to prevent parameter drift and improve robustness during adaptation. The neural network gain is selected as $kNN=100$. These parameters were determined experimentally through repeated simulations to achieve stable learning performance and effective uncertainty compensation.

With this structure, the RBFNN provides an adaptive compensation mechanism for unmodeled dynamics and lumped uncertainties, thereby enhancing the robustness and vibration suppression performance of the proposed control strategy.

3. Simulation results

Numerical simulations are carried out to evaluate the performance of the proposed control approach. The results obtained are then compared with several conventional control methods. The road disturbances considered in this study are illustrated in Figure 2 under two specific operating scenarios. In the first case, the road excitation is generated from white noise according to the ISO C-class road profile standard, with the vehicle traveling at v = 36km/h. In the second case, the vehicle moves at a higher speed, v = 54km/h, under a more severe excitation corresponding to the ISO D-class road profile. The effects of lumped uncertainties are also accounted for in both cases, with different uncertainty levels applied to each scenario. The technical specifications of the suspension system are listed in Table 1 below.

Table 1. Suspension specifications

Parameter	Value	Unit
m_s	320	kg
m_u	35	kg
k_s	25400	N/m
c_s	1950	Ns/m
k_t	165000	N/m

3.1. Performance under ISO C-class excitation

The variation of vehicle body motion under ISO C-class excitation is presented in Figure 3a. The simulation results show that the peak value and the RMS value of sprung mass displacement obtained by the passive suspension are 41.931mm and 15.148mm, respectively, which are significantly higher than those achieved by the active suspension system controlled by PID control (23.015mm and 9.470mm) and LQR control (20.992mm and 8.335mm). The proposed control strategy provides superior vibration suppression, reducing the vehicle body displacement to 10.074mm (peak) and 4.854mm (RMS).

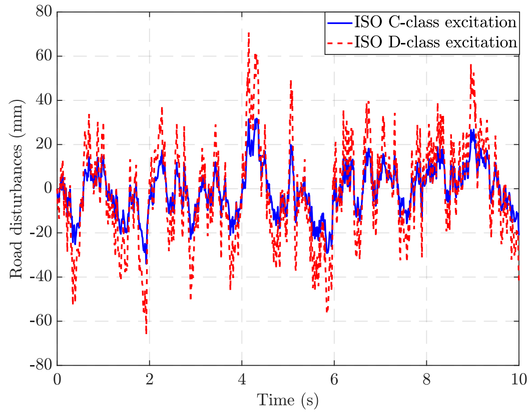

Figure 2. Road disturbances

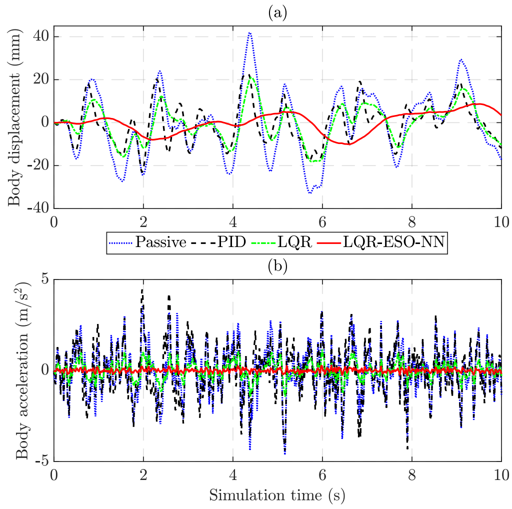

Figure 3. Vehicle body dynamics (1st case)

(a) Body displacement (b) Body acceleration

Ride comfort is evaluated through the variation of sprung mass acceleration. The results shown in Figure 3b indicate that the vehicle body acceleration obtained with the passive suspension and with the active suspension controlled by a PID controller are nearly identical, resulting in unsatisfactory ride comfort. In contrast, the LQR controller provides better vibration suppression, reducing the RMS acceleration to 0.445 m/s^2. A significant improvement is observed with the proposed control strategy, where the RMS acceleration is reduced to 0.093m/s^2, thereby improving ride comfort.

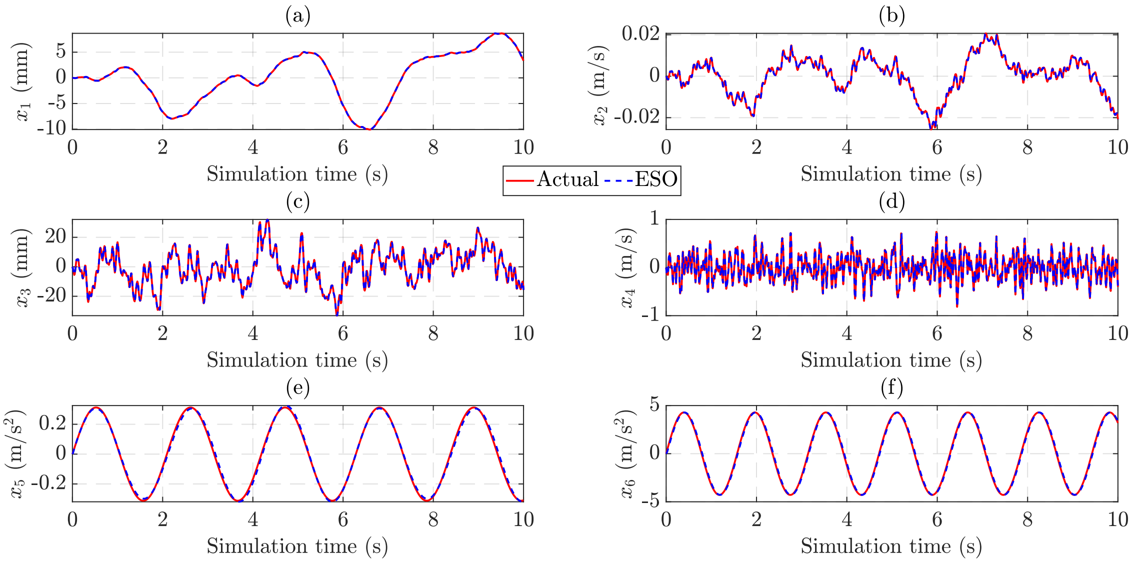

Figure 4. Observation errors (1st case)

(a) x_1; (b) x_2; (c) x_3; (d) x_4; (e) x_5; (f) x_6

The observation errors are illustrated in the subplots of Figure 4. It is clear that the signals estimated by the FOESO closely track the actual system states, with negligible errors. In terms of RMS values, the observation error of x_3 is only about 0.001mm, while that of x_4 is 0.001m/s. For the augmented states used to estimate the effects of lumped uncertainties, the observation errors for x_5 and x_6 are 0.013m/s^2 and 0.166m/s^2, respectively. These results confirm that the proposed control approach is highly effective at estimating the suspension system's dynamic states.

3.2. Performance under ISO D-class excitation

The second case investigates a more severe road excitation condition compared with the previous scenario. The simulation results in Figure 5a show that the vehicle body displacement can reach up to 71.261 mm when only the passive suspension system is employed. This value is significantly reduced to 41.678mm with PID control, 30.369mm with LQR control, and 14.693mm with the proposed control strategy when the active suspension system replaces the passive suspension. In terms of RMS values, the proposed control reduces sprung mass motion to 7.198mm, which is considerably lower than the values obtained with PID control (17.728mm) and LQR control (13.251mm).

Under stronger road excitation, the vehicle body acceleration exhibits significant variation. The results in Figure 5b show that the peak acceleration can exceed 10m/s^2 for both the passive suspension and the PID-controlled active suspension, whereas the proposed control strategy reduces the acceleration to no more than 0.736m/s^2. In terms of RMS values, the vehicle body acceleration achieved by the proposed control is only 0.220m/s^2, which is significantly lower than that obtained by LQR control (0.979m/s^2) and PID control (3.173m/s^2). This clearly demonstrates the superior performance of the proposed control strategy in vibration suppression and improved ride comfort.

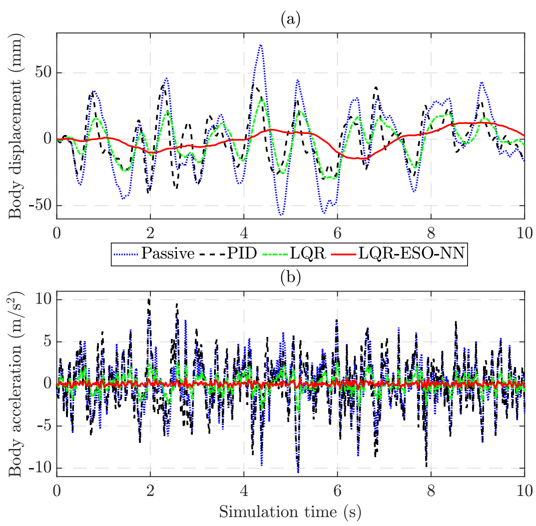

Figure 5. Vehicle body dynamics (2nd case)

(a) Body displacement (b) Body acceleration

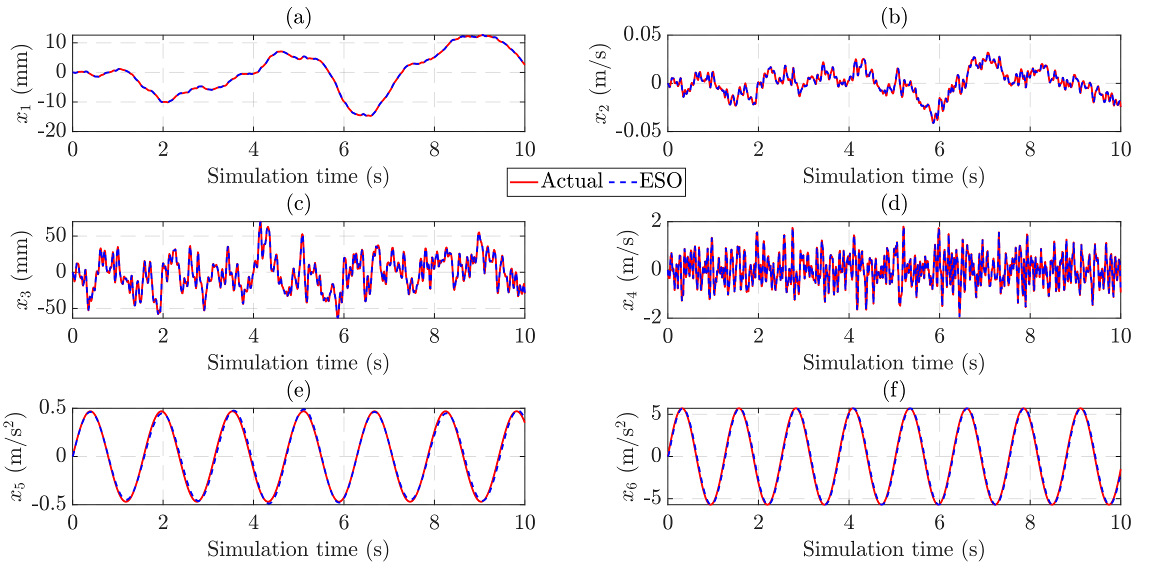

Figure 6. Observation errors (2nd case)

(a) x_1; (b) x_2; (c) x_3; (d) x_4; (e) x_5; (f) x_6

Although both road disturbances and lumped uncertainties increase considerably in the second scenario, the proposed observer still maintains high estimation accuracy for the system dynamics. The results in Figure 6 indicate that the RMS observation errors of x_3 and x_4 are only 0.002mm and 0.001m/s, respectively, while the observation errors of the augmented states are approximately 0.024m/s^2 for x_5 and 0.278m/s^2 for x_6.

The results obtained in both simulation scenarios consistently demonstrate that the proposed control strategy provides superior performance compared with conventional control methods in reducing vibration and improving ride comfort. In addition, the proposed FOESO accurately estimates the suspension system's dynamic states, thereby reducing implementation cost and improving signal quality.

Although the proposed control strategy combines FOESO and an adaptive RBFNN, the computational burden remains moderate because the LQR gain matrix is computed offline. At the same time, online computation mainly involves matrix operations, observer updating laws, and simple RBFNN adaptation laws with only five hidden neurons. Therefore, the proposed method is considered suitable for real-time implementation on automotive ECUs or embedded controllers.

4. Conclusion

A control scheme integrating LQR and an adaptive NN updating law has been developed in this study to improve the performance of the active suspension system. The FOESO is incorporated into the proposed control strategy to estimate the system's dynamic states, rather than relying on direct sensor measurements. Simulation results demonstrate that the proposed method is highly effective in enhancing ride comfort, even when the system is subjected to severe road disturbances and significant lumped uncertainties. The controller achieves superior vibration suppression compared with conventional methods, while the proposed FOESO provides accurate state estimation, thereby reducing implementation cost and improving signal quality.

However, some limitations remain, particularly in the selection and optimization of controller parameters and in the consideration of stronger nonlinearities in the suspension model. These issues will be further investigated in future work to improve the robustness and practical applicability of the proposed approach.

Acknowledgments

Tuan Anh Nguyen was funded by the PhD Scholarship Programme of Vingroup Innovation Foundation (VINIF), VinUniversity, code **VINIF.2025.TS77**.

REFERENCES

[1] M. H. A. Talib, et al. (2023), *Experimental evaluation of ride comfort performance for suspension system using PID and fuzzy logic*

controllers by advanced firefly algorithm, Journal of the Brazilian Society of Mechanical Sciences and Engineering, Vol.45.

[2] Le Van Duong, et al. (2023), *Comparison of controllers for nonlinear active suspension system*, Journal of Science and Technology - Hanoi University of Industry, Vol.59, No. 2A, pp.131-136.

[3] Tran Thi Thu Huong, Nguyen Tuan Anh, and Nguyen Manh Long (2022), *Simulation oscillation of active suspension system considering the effect of the hydraulic actuator*, Journal of Science and Technology - Danang University, Vol.20, No. 5, pp.23-26.

[4] Hoang Thang Binh, et al. (2024), *Research a hybrid PID controller for an active suspension system*, Journal of Science and Technology - Hanoi University of Industry, Vol.60, No. 6, pp.112-118.

[5] Vu Hai Quan and Le Huu Chuc (2020), *Simulation and control of active suspension for a full car model*, Journal of Science and Technology - Hanoi University of Industry, Vol.56, No. 2, pp.84-89.

[6] Nguyen Trong Duc, et al. (2021), *Modeling and analysis of active supply system for models vehicles using some different control methods*, Journal of Science and Technology - Hanoi University of Industry, Special Issue, Vol.11, 2021.

[7] Tran Van Da and Bui Duc Tien (2021), Controlling an active suspension system for four wheels car by combining LQR method and particle swarm optimization, Journal of Science and Technology - Hanoi University of Industry, Vol.57, No. 4, pp.85-88.

[8] Vu Hai Quan, Nguyen Anh Ngoc, and Nguyen Huy Truong (2021), *Dynamic analysis of active suspension system for 1/4 model vehicle using PID and LQR controller*, Journal of Marine Science and Technology, Special Issue, pp.229-233.

Received:	12/05/2026
Revised:	21/05/2026
Accepted:	22/05/2026